Liquid Crystals

Publication details, including instructions for authors and subscription information:
http://www.informaworld.com/smpp/title~content=t713926090

Unsymmetrical dimers possessing a cholesteryl ester moiety and a difluoro-substituted biphenyl core: synthesis and mesomorphic behaviour

C. V. Yelamaggad[a]; Manoj Mathews[a]
[a] Centre for Liquid Crystal Research, P. B. No. 1329, Jalahalli, Bangalore 560 013, India,

To cite this Article Yelamaggad, C. V. and Mathews, Manoj(2003) 'Unsymmetrical dimers possessing a cholesteryl ester moiety and a difluoro-substituted biphenyl core: synthesis and mesomorphic behaviour', Liquid Crystals, 30: 2, 125 — 133

To link to this Article: DOI: 10.1080/0267829021000060179

URL: http://dx.doi.org/10.1080/0267829021000060179

Liquid Crystals, 2003, Vol. 30, No. 2, 125–133

Taylor & Francis
Taylor & Francis Group

Unsymmetrical dimers possessing a cholesteryl ester moiety and a difluoro-substituted biphenyl core: synthesis and mesomorphic behaviour

C. V. YELAMAGGAD* and MANOJ MATHEWS
Centre for Liquid Crystal Research, P. B. No. 1329, Jalahalli, Bangalore 560 013, India

(*Received 15 June 2002; in final form 30 August 2002; accepted 10 September 2002*)

Some new unsymmetrical dimers consisting of a cholesteryl ester moiety, covalently linked to either a 4′-(2,3-difluoro-4-*n*-octyloxy)biphenyloxy or a 4′-(2,3-difluoro-4-*n*-decyloxy)biphenyloxy through odd–even parity paraffinic central spacers, have been synthesized and investigated for their mesomorphic behaviour. Except for one, all the dimers exhibit enantiotropic smectic A, twist grain boundary (TGB) and chiral nematic mesophases. Five of the eight unsymmetrical dimers synthesized show a chiral smectic C (SmC*) phase. Interestingly in some of the compounds the SmC* exists over a wide temperature range including room temperature. Among the eight compounds, a dimer having a C_7 central paraffinic spacer and a C_8 alkoxy terminal chain shows an enantiotropic twist grain boundary with SmC* blocks (TGB_{C^*}) phase. It appears that the variation in the length of the spacer has a remarkable influence on the phase transition temperatures as well as on the mesomorphic behaviour.

1. Introduction

Liquid crystalline dimers (also known as dimesogens) composed of either indentical (symmetrical) or non-identical (unsymmetrical) mesogenic segments, connected through a flexible paraffinic central spacer, are attracting a great deal of attention. This is because the symmetrical dimers are regarded as model compounds for polymeric liquid crystals [1], while the unsymmetrical dimers exhibit a novel family of smectic phases [1–6]. Moreover, chiral unsymmetrical dimers, in particular compounds possessing a cholesteryl ester unit as the chiral entity joined to different aromatic mesogens through an alkylene spacer, show interesting thermal behaviour. For example, we have recently reported that an unsymmetrical dimer formed by joining a cholesteryl ester moiety to a 4-*n*-hexyloxytolan core through a *n*-pentyl (C_5) spacer exhibits a reentrant twist grain boundary (with smectic A blocks, TGB_A) phase, including a newly discovered twist grain boundary (with smectic C* blocks, TGB_{C^*}) phase [4*a*]. When an achiral or chiral tolan (diphenylacetylene) entity is attached to a cholesteryl ester unit via a *n*-pentyl spacer, the resulting unsymmetrical dimer stabilizes the chiral nematic (N*) [4*b*, *c*] or SmA mesophases (showing an electroclinic effect) over a wide temperature range [4*d*].

Hardouin *et al* have reported reentrant incommensurate smectic A (SmA_{ic}) and chiral smectic C (SmC*) mesophases in an unsymmetrical dimer formed by joining a cholesteryl ester moiety to a schiff's base through a *n*-pentyl (C_5) spacer [5*b*]. Further studies on similar type of compound showed that the length of the spacer and the molecular structure of the non-cholesteryl mesogenic (aromatic) segment are more important for the occurrence of an incommensurate phase than for the appearance of other mesophases, viz the blue phases (BP), the TGB phase and the SmC* phase [5*c*–*e*]. In an effort to stabilize similar mesophases we have explored the possibility of attaching different types of chiral or achiral schiffs base entities to the cholesteryl ester unit through an *n*-pentyl spacer. These dimers exhibit SmA, TGB and N* mesophases [6] indicating the sensitivity of mesomorphic behaviour to the structure of the aromatic (non-cholesteryl) mesogenic segment in these systems. Thus in order to understand the structure–property relations a variety of unsymmetrical dimers possessing a cholesteryl ester unit as the chiral entity joined to other aromatic mesogens such as biphenyl, salicylaldimine, tolan, schiffs base, azo, stilbene, ester, etc., have been synthesized and investigated for their thermal behaviour. Although no general conclusion could be inferred on the structure–property relation, it appears that the unsymmetrical dimers with an odd-parity alkylene spacer exhibit unusual thermal behaviour, as evident from many research articles.

It is now well documented that fluoro-substitution in liquid crystalline materials helps in modifying properties

*Author for correspondence; e-mail: clcr@vsnl.com

Liquid Crystals ISSN 0267-8292 print/ISSN 1366-5855 online © 2003 Taylor & Francis Ltd
http://www.tandf.co.uk/journals
DOI: 10.1080/0267829021000060179

such as melting point, transition temperature, mesophase type and other physical properties of a parent system [7, 8]. In general fluoro-substitution can be made at different positions within the aromatic core, the terminal chains or the linking groups, with an associated widely varying thermal behaviour [7]. The number of fluorine atoms substituted over the aromatic mesogenic core usually varies from one to two, but in some cases can be up to five [7]. In the case of disubstituted fluoro compounds the thermal behaviour of a liquid crystal depends not only upon their relative positions but also on the molecular structure of the aromatic cores (e.g. terphenyl, biphenyl, pyridine, pyridazine, etc.) to which they are attached [7]. Lateral fluoro-substitutions have long been used to generate a lateral dipole because of the small fluorine atom size and high electronegativity, serving to minimize viscosity. Gray *et al.* have reported that 2,3-difluorobiphenyls having either an alkyl or an alkoxy terminal tail exhibit smectic phases with much lower transition temperatures [8 *a*]. Among these, 2,3-difluoro-4′-heptyl-4-octyloxybiphenyl shows significant polar character and large dielectric anisotropy because the two fluoro substituents are closer to the ether oxygen. In view of these observations, and to understand the structure–property relation, here we report the synthesis and characterization of the first unsymmetrical dimers consisting of 2,3-difluoro-4-octyl/decyloxybiphenyl connected to a cholesteryl ester moiety through either even (C_4) or odd (C_3, C_5 and C_7) alkylene spacers.

2. Experimental

2.1. *General*

Cholesterol, tetrakis(triphenylphosphine)palladium(0), 8-bromooctanoic acid, 6-bromohexanioc acid, 5-bromovaleric acid, 4-bromobutyric acid, 2,3-difluorophenol and 1-bromoalkanes were obtained from Aldrich. The crude target molecules and some intermediates obtained have been purified by column chromatography using neutral aluminium oxide as a stationary phase. Thin layer chromatography (TLC) was performed on aluminium sheets pre-coated with silica gel (Merck, Kieselge 60, F_{254}). IR spectra were recorded using a Perkin Elmer Spectrum 1000 FTIR spectrometer. ^{1}H NMR spectra were recorded using either a Bruker AMX-400 (400 MHz) or Bruker Aveance series DPX-200 (200 MHz) spectrometers; the chemical shifts are reported in parts per million (ppm) relative to tetramethylsilane (TMS) as an internal standard. Mass spectra were recorded on a Jeol JMS-600H spectrometer. Microanalyses were obtained with the help of a Eurovector model EA 3000 elemental analyser. The identification of the mesophases and the transition temperatures of the compounds were determined using a polarizing microscope (Leitz DMRXP) in conjunction with a programmable hot stage (Mettler FP90). Phase transition enthalpy was measured using a differential scanning calorimeter (Perkin Elmer DSC7). Optical observations were made using either clean untreated glass slides or slides treated for homogeneous or for homeotropic alignment of the molecules.

2.2. *Synthesis and molecular structural characterization*

The unsymmetrical dimers and the intermediates were synthesized as outlined in the scheme. The intermediates 1,2-difluoro-3-alkoxybenzenes **6a** or **6b** and the corresponding arylboronic acids **5a** or **5b** were synthesized following procedures reported in the literature [8 *a*, *e*].

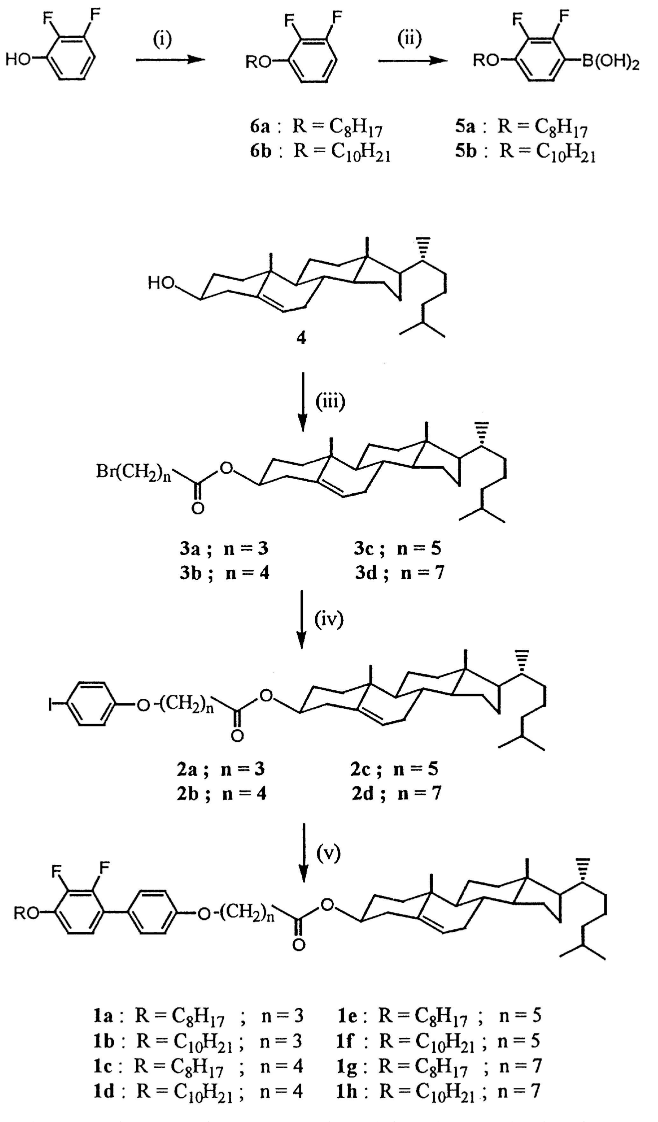

Scheme. A general route employed for the synthesis of symmetrical dimers. Reagents and conditions: (i) anhyd.K_2CO_3, 1-*n*-bromooctane/decane, acetone, reflux, 24 h; (ii) *n*-BuLi, $[(CH3)_2CHO]_3B$, −78°C, aqueous HCl; (iii) bromoalkanoyl chlorides, pyridine-THF, rt, 24 h; (iv) 4-iodophenol, anhyd.K_2CO_3, 2-butanone, 70°C, 24 h; (v) **5a** or **5b**, $[(C_6H_5)_3P]_4Pd$, Na_2CO_3, ethanol, benzene, reflux, 30 h.

Cholesteryl bromoalkanoates (**3a**–**d**) were prepared by esterification of commercial optically pure cholesterol with alkanoyl chlorides as described in [2, 5]. The key intermediates, cholesteryl iodo compounds **2a**–**d** were prepared by reacting 4-iodophenol and cholesteryl bromoalkanoates in the presence of a mild base [5*d*]. Palladium cross-coupling reaction involving boronic acids **5a**, **b** and cholesteryl iodo compounds **2a**–**d** furnished the target molecules in 64–92% yield.

The molecular structures of the intermediates and unsymmetrical dimers (**1a**–**d**) were confirmed with the help of spectroscopic analysis. The spectral data of all the intermediates and unsymmetrical dimers were found to be consistent with their proposed molecular structure. The IR and ^{1}H spectrum of all the unsymmetrical dimers appear similar. The IR spectra show absorption bands in the region of ν_{max} 2857–2951 and 1719–1743 cm^{-1} due to C–H (paraffinic) and carbonyl (C=O of ester) stretching vibrations, respectively. In the ^{1}H NMR spectra, six aromatic protons appear in the form of four patterns namely, a doublet (d), a doublet of triplet (dt), a doublet and a multiplet (m) in the region δ 7.4–7.42, 7.03–7.04, 6.94–6.95 and 6.76–6.77 respectively. The olefinic, methine of an ester, and the oxymethylene of paraffinic chain protons resonate in the region δ 5.33–5.37, 4.6–4.63 and 4.04–4.06 as a broad d, m and m, respectively. The ^{13}C NMR spectra are presented for the samples **1a** and **1d** as representative cases. We discuss the ^{13}C NMR spectra, especially the signals obtained at higher frequency, for the compound **1a**. The C=O carbon resonates at δ 172.58 whereas the two carbons of the biphenyl core bearing fluoro-substitution appear as two sets of doublet of doublet (dd) at δ 148.86 and 142.01. The adjacent carbons of the carbons bearing fluoro-substitution resonate as d each at δ 147.51 and 122.85. The quaternary (C) and tertiary carbon (CH) of the double bond resonate at δ 139.71 and 122.71, respectively. The remaining signals resonating at δ 158.56, 129.88, 127.47, 123.3, 114.67 and 109.79 are due to other aromatic carbons, and lower frequency signals are found to be consistent with the proposed structure.

2.2.1. *Cholesteryl [4′-(2,3-difluoro-4-n-octyl/decyloxy)biphenyloxy]alkanoates* ***1a*–*h***

These unsymmetrical dimers were prepared following a general synthetic procedure. Thus, to a magnetically stirred suspension of cholesteryl (4-iodophenoxy)alkanoates (**2a**–**d**) (0.6 mmol, 1 equiv.), 2,3-difluoro-4-octyloxy/decyloxyphenylboronic acid (**5a**/**5b**) (0.7 mmol, 1.17 equiv.), tetrakis(triphenylphosphine)palladium(0) (30 mg), in a mixture of ethanol (5 ml) and benzene (3 ml), to which was added a solution of aqueous sodium carbonate solution (2M, 2 ml) at room temperature (rt). After degassing and introducing argon gas, the reaction mixture was heated to reflux for 12 h. The reaction mixture was cooled to rt, diluted with water and extracted with CH_2Cl_2 (10 ml × 2). The organic layer was washed with water (100 ml × 2), brine and dried over anhyd. Na_2SO_4. Evaporation of the solvent furnished a pale yellow solid that was purified by column chromatography using neutral alumina as a stationary phase. Elution with a mixture of 5% EtOAc/hexanes furnished a white solid which was further purified by repeated recrystallizations (4 times) in a mixture of absolute ethanol/CH_2Cl_2 (9/1).

Cholesteryl 4-[4′-(2,3-difluoro-4-n-octyloxy)biphenyloxy]butanoate ***1a***: $R_f = 0.4$ (10% EtOAc/hexanes), white solid, yield 0.3 g (64%). IR (KBr pellet): ν_{max} 2936, 1719, 1672, 1612, 1572 and 1505 cm^{-1}. ^{1}H NMR ($CDCl_3$, 400 MHz): 7.42 (dd, $J = 8.68$ Hz, $J = 1.44$ Hz, 2H, Ar), 7.04 (d of t, $J = 8.48$ Hz, $J = 2.32$ Hz, 1H, Ar), 6.94 (d, $J = 8.8$ Hz, 2H, Ar), 6.77 (m, 1H, Ar), 5.37 (br d, $J = 3.92$ Hz, 1H, olefinic), 4.63 (m, 1H, CHOCO), 4.05 (m, 4H, 2 × OCH_2), 2.5–2.32 (m, 4H, 2 × allylic methylene), 1.98–0.96 (m, 46H, 17 × CH_2, 6 × CH, 2 × CH_3), 1.00 (s, 3H, 1 × CH_3), 0.86 (d, $J = 1.76$ Hz, 3H, 1 × CH_3), 0.85 (d, $J = 1.76$ Hz, 3H, 1 × CH_3) and 0.67 (s, 3H, 1 × CH_3). ^{13}C NMR (100 MHz, $CDCl_3$): 172.58, 158.56, 148.86 (dd, $^1J_{C\text{-}F} = 243$ Hz, $^2J_{C\text{-}F} = 10.8$ Hz), 147.51 (d, $^2J_{C\text{-}F} = 9.6$ Hz), 142.01 (dd, $^1J_{C\text{-}F} = 245$ Hz, $^2J_{C\text{-}F} = 14.4$ Hz), 139.71, 129.88, 127.47, 123.3, 122.85 (d, $^2J_{C\text{-}F} = 10.9$ Hz), 122.71, 114.67, 109.79, 74.14, 70.08, 66.95, 56.77, 56.24, 50.13, 42.39, 39.81, 39.58, 38.21, 37.06, 36.66, 36.25, 35.83, 31.95, 31.83, 31.19, 29.32, 29.24, 28.26, 28.05, 27.87, 25.92, 24.79, 24.32, 23.89, 22.83, 22.67, 22.59, 21.09, 19.34, 18.77, 14.1 and 11.9%. FAB Mass: 787.8 $[M]^+$. Elemental analysis: calc. for $C_{51}H_{74}F_2O_4$, C 77.62, H 9.45; found C 77.8, H 9.28%.

Cholesteryl 4-[4′-(2,3-difluoro-4-n-decyloxy)biphenyloxy]butanoate ***1b***: $R_f = 0.42$ (10% EtOAc/hexanes), white solid, yield 0.37 g (83%). IR (KBr pellet): ν_{max} 2935, 1735, 1671, 1631, 1572 and 1507 cm^{-1}. ^{1}H NMR ($CDCl_3$, 400 MHz): 7.41 (d, $J = 7.32$ Hz, 2H, Ar), 7.03 (t, $J = 8.36$ Hz, 1H, Ar), 6.95 (d, $J = 8.56$ Hz, 2H, Ar), 6.77 (t, $J = 7.94$ Hz, 1H, Ar), 5.37 (brd, $J = 3.92$ Hz, 1H, olefinic), 4.63 (m, 1H, CHOCO), 4.05 (m, 4H, 2 × OCH_2), 2.5–2.32 (m, 4H, 2 × allylic methylene), 2.15–1.03 (m, 50H, 19 × CH_2, 6 × CH, 2 × CH_3), 1.00 (s, 3H, 1 × CH_3), 0.86 (d, $J = 4$ Hz, 6H, 2 × CH_3), and 0.66 (s, 3H, 1 × CH_3). FAB Mass: 815.4 $[M]^+$. Elemental analysis: calc. for $C_{53}H_{78}F_2O_4$, C 77.9, H 9.62; found C 77.75, H 10.26%.

Cholesteryl 5-[4′-(2,3-difluoro-4-n-octyloxy)biphenyloxy]pentanoate ***1c***: $R_f = 0.4$ (10% EtOAc/hexanes), white solid, yield 0.28 g (58%). IR (KBr pellet): ν_{max} 2940, 1736, 1665, 1630, 1586 and 1504 cm^{-1}. ^{1}H NMR ($CDCl_3$, 400 MHz): 7.41 (d, $J = 7.32$ Hz, 2H, Ar), 7.04 (d of t,

$J = 8.44$ Hz, $J = 2.28$ Hz, 1H, Ar), 6.94 (d, $J = 8.72$ Hz, 2H, Ar), 6.76 (m, 1H, Ar), 5.35 (brd, $J = 3.92$ Hz, 1H, olefinic), 4.61 (m, 1H, CHOCO), 4.04 (m, 4H, $2 \times OCH_2$), 2.4–2.25 (m, 4H, 2 × allylic methylene), 1.98–0.96 (m, 48H, $18 \times CH_2$, $6 \times CH$, $2 \times CH_3$), 1.00 (s, 3H, $1 \times CH_3$), 0.87 (d, $J = 1.64$ Hz, 3H, $1 \times CH_3$), 0.85 (d, $J = 1.72$ Hz, 3H, $1 \times CH_3$) and 0.67 (s, 3H, $1 \times CH_3$). FAB Mass: 802.4 $[M]^+$. Elemental analysis: calc. for $C_{52}H_{76}F_2O_4$, C 77.76, H 9.54; found C 77.54, H 10.15%.

Cholesteryl 5-[4′-(2,3-difluoro-4-n-decyloxy)biphenyloxy]pentanoate ***1d***: $R_f = 0.42$ (10% EtOAc/hexanes), white solid, yield 0.4 g (88%). IR (KBr pellet): ν_{max} 2928, 1743, 1608 and 1503 cm^{-1}. ^1H NMR ($CDCl_3$, 400 MHz): 7.41 (d, $J = 8.04$ Hz, 2H, Ar), 7.04 (t, $J = 7.44$ Hz, 1H, Ar), 6.94 (d, $J = 8.6$ Hz, 2H, Ar), 6.76 (t, $J = 7.82$ Hz, 1H, Ar), 5.33 (brd, $J = 3.92$ Hz, 1H, olefinic), 4.62 (m, 1H, CHOCO), 4.05 (m, 4H, $2 \times OCH_2$), 2.4–2.25 (m, 4H, 2 × allylic methylene), 2.01–1.05 (m, 52H, $20 \times CH_2$, $6 \times CH$, $2 \times CH_3$), 1.00 (s, 3H, $1 \times CH_3$), 0.86 (d, $J = 4.01$ Hz, 6H, $2 \times CH_3$), and 0.66 (s, 3H, $1 \times CH_3$). ^{13}C NMR (100 MHz, $CDCl_3$): 172.84, 158.64, 148.86 (dd, $^1J_{C\text{-}F} = 247$ Hz, $^2J_{C\text{-}F} = 11$ Hz), 147.5 (d, $^2J_{C\text{-}F} = 11.4$ Hz), 142.0 (dd, $^1J_{C\text{-}F} = 245$ Hz, $^2J_{C\text{-}F} = 14.7$ Hz), 139.73, 129.86, 127.34, 123.28, 122.8 (d, $^2J_{C\text{-}F} = 10.9$ Hz), 122.68, 114.65, 109.76, 73.97, 70.06, 67.52, 56.77, 56.24, 50.12, 42.38, 39.81, 39.58, 38.22, 37.06, 36.66, 36.26, 35.84, 34.33, 29.58, 29.36, 29.25, 28.71, 28.26, 28.05, 27.88, 25.93, 24.33, 23.89, 22.84, 22.71, 22.59, 21.79, 21.09, 19.34, 18.77, 14.1 and 11.9. FAB Mass: 829.9 $[M]^+$ ($C_{54}H_{80}F_2O_4$).

Cholesteryl 6-[4′-(2,3-difluoro-4-n-octyloxy)biphenyloxy]hexanoate ***1e***: $R_f = 0.48$ (10% EtOAc/hexanes), white solid, yield 0.34 g (78%). IR (KBr pellet): ν_{max} 2942, 1731, 1671, 1610, 1570 and 1504 cm^{-1}. ^1H NMR ($CDCl_3$, 400 MHz): 7.42 (dd, $J = 7.24$ Hz, $J = 1.4$ Hz, 2H, Ar), 7.04 (d of t, $J = 8.44$ Hz, $J = 2.28$ Hz, 1H, Ar), 6.94 (d, $J = 8.76$ Hz, 2H, Ar), 6.76 (m, 1H, Ar), 5.37 (brd, $J = 3.92$ Hz, 1H, olefinic), 4.61 (m, 1H, CHOCO), 4.05 (m, 2H, $1 \times OCH_2$), 3.99 (m, 2H, $1 \times OCH_2$), 2.38–2.27 (m, 4H, 2 × allylic methylene), 1.98–0.96 (m, 50H, $18 \times CH_2$, $6 \times CH$, $2 \times CH_3$), 1.00 (s, 3H, $1 \times CH_3$), 0.87 (d, $J = 1.76$ Hz, 3H, $1 \times CH_3$), 0.85 (d, $J = 1.80$ Hz, 3H, $1 \times CH_3$) and 0.66 (s, 3H, $1 \times CH_3$). FAB Mass: 817.2 $[M]^+$ ($C_{53}H_{78}F_2O_4$).

Cholesteryl 6-[4′-(2,3-difluoro-4-n-decyloxy)biphenyloxy]hexanoate ***1f***: $R_f = 0.44$ (10% EtOAc/hexanes), white solid, yield 0.42 g (quantitative). IR (KBr pellet): ν_{max} 2951, 1731, 1608 and 1504 cm^{-1}. ^1H NMR ($CDCl_3$, 400 MHz): 7.40 (d, $J = 7.32$ Hz, 2H, Ar), 7.04 (d of t, $J = 8.56$ Hz, $J = 2.36$ Hz, 1H, Ar), 6.94 (d, $J = 8.8$ Hz, 2H, Ar), 6.76 (t, $J = 8.2$ Hz, 1H, Ar), 5.37 (brd, $J = 4.2$ Hz, 1H, olefinic), 4.61 (m, 1H, CHOCO), 4.06 (t, $J = 8$ Hz, 2H, $1 \times OCH_2$), 3.98 (t, $J = 6.36$ Hz, 2H, $1 \times OCH_2$), 2.38–2.27 (m, 4H, 2 × allylic methylene), 2.01–1.05 (m, 54H, $21 \times CH_2$, $6 \times CH$, $2 \times CH_3$), 1.00 (s, 3H, $1 \times CH_3$), 0.87 (d, $J = 1.84$ Hz, 3H, $1 \times CH_3$), 0.85 (d, $J = 1.8$ Hz, 3H, $1 \times CH_3$) and 0.66 (s, 3H, $1 \times CH_3$). FAB Mass: 843.9 $[M]^+$. Elemental analysis: calc. for $C_{55}H_{82}F_2O_4$, C 78.15, H 9.78; found C 77.70, H 10.11%.

Cholesteryl 8-[4′-(2,3-difluoro-4-n-octyloxy)biphenyloxy]octanoate ***1g***: $R_f = 0.48$ (10% EtOAc/hexanes), white solid, yield 0.32 g (63%). IR (KBr pellet): ν_{max} 2935, 1735, 1671, 1631, 1572 and 1507 cm^{-1}. ^1H NMR ($CDCl_3$, 400 MHz): 7.41 (d, $J = 7.32$ Hz, 2H, Ar), 7.04 (d of t, $J = 8.43$ Hz, $J = 2.18$ Hz, 1H, Ar), 6.94 (d, $J = 8.72$ Hz, 2H, Ar), 6.76 (m, 1H, Ar), 5.37 (brd, $J = 3.92$ Hz, 1H, olefinic), 4.61 (m, 1H, CHOCO), 4.05 (t, $J = 6.58$ Hz, 2H, $1 \times OCH_2$), 3.98 (t, $J = 6.48$ Hz, 2H, $1 \times OCH_2$), 2.31–2.26 (m, 4H, 2 × allylic methylene), 2.01–0.96 (m, 54H, $21 \times CH_2$, $6 \times CH$, $2 \times CH_3$), 1.00 (s, 3H, $1 \times CH_3$), 0.87 (d, $J = 1.76$ Hz, 3H, $1 \times CH_3$), 0.85 (d, $J = 1.80$ Hz, 3H, $1 \times CH_3$) and 0.66 (s, 3H, $1 \times CH_3$). FAB Mass: 844.1 $[M]^+$. Elemental analysis: calc. for $C_{55}H_{82}F_2O_4$, C 78.15, H 10.55; found C 78.68, H 10.28%.

Cholesteryl 8-[4′-(2,3-difluoro-4-n-decyloxy)biphenyloxy]octanoate ***1h***: $R_f = 0.5$ (10% EtOAc/hexanes), white solid, yield 0.37 g (87%). IR (KBr pellet): ν_{max} 2928, 1719, 1608 and 1504 cm^{-1}. ^1H NMR ($CDCl_3$, 400 MHz): 7.41 (d, $J = 7.32$ Hz, 2H, Ar), 7.04 (d of t, $J = 8.36$ Hz, $J = 2.04$ Hz, 1H, Ar), 6.95 (d, $J = 8.8$ Hz, 2H, Ar), 6.77 (t, $J = 7.32$ Hz, 1H, Ar), 5.36 (brd, $J = 4.2$ Hz, 1H, olefinic), 4.60 (m, 1H, CHOCO), 4.06 (t, $J = 6.6$ Hz, 2H, $1 \times OCH_2$), 3.98 (t, $J = 6.52$ Hz, 2H, $1 \times OCH_2$), 2.31–2.26 (m, 4H, 2 × allylic methylene), 2.01–1.03 (m, 58H, $23 \times CH_2$, $6 \times CH$, $2 \times CH_3$), 1.00 (s, 3H, $1 \times CH_3$), 0.87 (d, $J = 1.84$ Hz, 3H, $1 \times CH_3$), 0.85 (d, $J = 1.8$ Hz, 3H, $1 \times CH_3$) and 0.66 (s, 3H, $1 \times CH_3$). FAB Mass: 872.3: $[M]^+$ ($C_{57}H_{86}F_2O_4$).

3. Results and discussion

The table shows the phase sequence, transition temperatures and associated enthalpies of the unsymmetrical dimers realized in the present investigation. For a comparative study, and to understand structure–property relations the length of both the terminal alkoxy chain (C_8 and C_{10}) and the central alkylene spacer (C_3, C_4, C_5 and C_7) have been varied. The dimer **1a** having a C_3 spacer and C_8 terminal alkoxy chain exhibits enantiotropic SmA, TGB and N* mesophases in addition to a monotropic SmC* phase. The SmA phase was identified by the observation of focal-conic texture in slides treated for planar orientation, and a dark field of view in slides treated for homeotropic orientation. In the N* mesophase oily streak texture was observed which on slight

Table. Transition temperatures[a] (°C) and enthalpies (J gm^{-1}) (in brackets) of dimesogens. The enthalpy values are enclosed in brackets. I = isotropic liquid state; N* = chiral nematic phase; TGB = twist grain boundary; SmA = smectic A phase; SmC* = chiral smectic C phase; TGB$_{C*}$ = twist grain boundary with smectic C* blocks phase; Cr = Crystal.

Dimesogen	Cr	Heating Cooling	TGB$_{C*}$	Heating[c] Cooling	SmC*	Heating[c] Cooling	SmA	Heating Cooling	TGB	Heating Cooling	N*	Heating Cooling	I
1a	•	127 (47.5)	—		•	—	•	177.1 (2.5)	•	[d]	•	179.9 (4.1)	•
		49.4 (16.7)				92.8		176.4 (2.4)				179.04 (4.6)	
1b	•	81.4 (44.4)	—		•	105.8	•	174.3 (10.7)	—		—		•
						104.7		171.5 (6.3)					
1c	•	80.1 (45.4)	—		—		•	119.7 (1)	•	[d]	•	125.5 (0.7)	•
								119.1 (0.7)				125.0 (0.8)	
1d	•	83.4 (47.1)	—		—		•	121 (2.2)	•	[d]	•	121.7 (0.7)	•
		65.9 (42.4)						120.4 (2.2)				121.3 (0.6)	
1e	•	67.4[b] (20.3)	—		•	92.5	•	151.2 (0.7)	•	[d]	•	161.1 (4.3)	•
						91.5		150.6 (0.9)				159.8 (4.4)	
1f	•	62.1 (36.9)	—		•	103.6	•	154.9 (2.5)	•	[d]	•	156.8 (4.1)	•
						101.8		153.5 (1.6)				155.3 (2.9)	
1g	•	77.1[b] (19.4)	•	85.8	—		•	117.5[c]	•	124.0 (0.6)	•	145.0 (4.1)	•
				84.9				115.6[c]		123.6 (0.4)		143.9 (4.6)	
1h	•	101.9 (41.8)	—		•	—	•	132.4 (0.6)	•	[d]	•	142 (4.4)	•
						94.2		130.6 (0.6)				139.9 (4.6)	

[a] Peak temperatures in the DSC thermograms obtained during the first heating and cooling cycles at 5° min^{-1}.

[b] An additional crystal to crystal transition has been observed for the compounds **1e** and **1g** at 73.6 and 63.7 (15.2) 56.7°C (11.2) respectively.

[c] The phase transition was observed under polarizing microscope; it was too weak to be recognized in DSC.

[d] TGB is a transient phase.

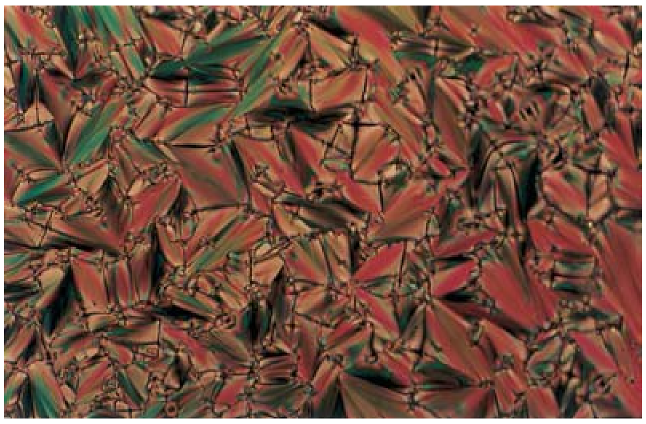

Figure 1. Photomicrograph of the optical texture observed at 110.1°C for the SmA phase while cooling from the isotropic phase of dimer **1b**.

shear changed to planar texture. The TGB phase showed the filament texture when the substrate was treated for homeotropic alignment. The N* and SmA phases coexisted with the TGB phase which was evident from the fact that the textures corresponding to these three mesophases appeared simultaneously for a short while indicating the existence of the TGB phase over a narrow temperature range. In slides treated for planar orientation the SmC* phase exhibited dechiralization lines on top of the focal-conic fan texture phase, while with the surfaces treated for homeotropic alignment a cloudy texture was observed when the sample was cooled from the SmA phase.

The dimer **1b**, the higher homologue of **1a**, having a C_{10} terminal alkoxy chain, showed enantiotropic SmC* and SmA phases only. The focal-conic textures seen in the SmA and SmC* phases are shown in figures 1 and 2, respectively. During the first cooling of the compound from the SmC* phase a step-like variation occurs at $-8.7°C$ ($\Delta H = 2.5\ \mathrm{J\ g^{-1}}$) which can be attributed to a transition from SmC* to either a glassy state or to another mesophase, which exists down to $-40°C$. Thus the SmC* phase exists over a wide temperature range. With the existing experimental set-up it was not possible for us to confirm the nature of the phase stabilized below $-8.7°C$. On subsequent heating, step-like variation appears again at about 3.1°C ($\Delta H = 1\ \mathrm{J\ g^{-1}}$) and on further heating the compound crystallizes at ~42°C ($\Delta H = 8\ \mathrm{J\ g^{-1}}$). The absence of TGB and N* phases, and the enantiotropic nature of the SmC* phase, in this dimer clearly indicate the influence of the length of terminal alkoxy chain on the structure–property relationship. The dimers **1c** and **1d**, both having a C_4 central alkylene spacer but differing in the length of terminal alkoxy chain C_8 and C_{10}, respectively, show SmA, TGB and N* phases. In both the cases the crystal melting and isotropic temperatures are much lower than the values for other members. We show the DSC traces for the first heating and subsequent cooling cycles obtained at a rate of 5°C min^{-1} for **1c** (figure 3). Notice that in the cooling cycle the SmA phase supercools till $-40°C$. Both **1c** and **1d** compounds show similar thermal behaviour except that sample **1d** crystallizes at about 66°C, while crystallization does not occur even till $-40°C$ in case of **1c**.

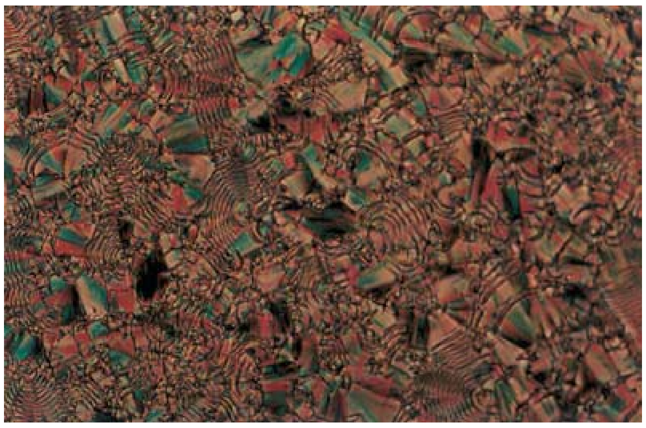

Figure 2. Photomicrograph of the optical texture observed at 87.1°C for the SmC* while cooling from the SmA phase of dimer **1b**.

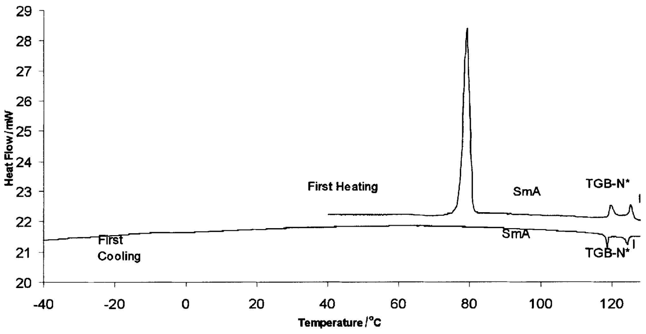

Figure 3. DSC thermograms obtained at a rate of 5°C min^{-1} for the compound **1c** during first heating and subsequent cooling cycles.

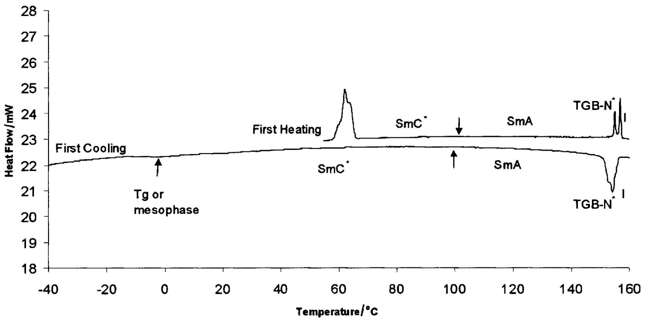

Figure 4. DSC thermograms obtained for the first heating and cooling cycles at a rate of 5°C min^{-1} for the compound **1f**.

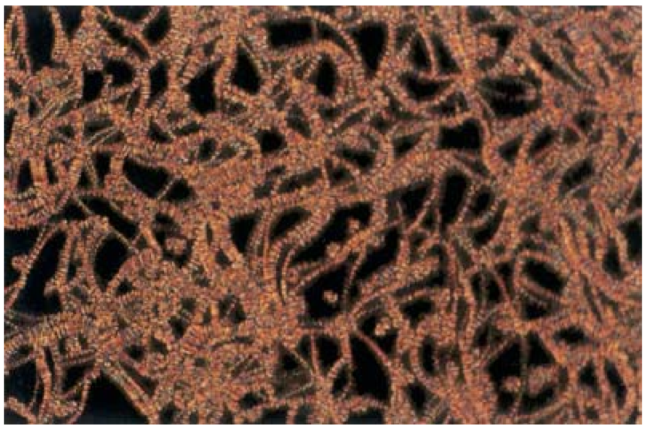

Figure 5. Photomicrograph of the undulated filament texture obtained in the TGB_{C*} phase at 82.5°C while cooling from the SmA phase of the unsymmetrical dimer **1g** with homeotropic orientation.

The unsymmetrical dimers **1e** and **1f**, containing a C_5 central alkylene spacer but differing in the length of terminal alkoxy tail C_8 and C_{10}, respectively, exhibit enantiotropic SmC*, SmA, TGB and N* phases. The dimer **1e**, on cooling from the SmA phase, exhibits a SmC* phase between 91.5 and -1°C. Around -1°C a step-like variation has been observed having $\Delta H = 0.52\ \mathrm{J\ g^{-1}}$. Thus the SmC* phase exists over a wide temperature range. The phase appearing below -1°C exists till -40°C but owing to experimental limitations we have been unable to characterize it. The unsymmetrical dimer **1f** on cooling shows a SmC* phase at 101.8°C which exists till -2.7°C ($\Delta H = 0.48\ \mathrm{J\ g^{-1}}$) indicating the stabilization of this phase over a 100°C temperature range (figure 4). On subsequent heating a small rounded peak appears (at -2.8°C, $\Delta H = 0.6\ \mathrm{J\ g^{-1}}$) and on further heating the compound shows no sign of crystallization. Needless to say, both the compounds show similar thermal behaviour and there seems to be no influence of the length of the terminal alkoxy chain on the mesomorphic behaviour.

Figure 6. Photomicrograph obtained in the TGB_{C*} phase at 83°C while cooling from the SmA phase of the dimer **1g**, in planar orientation; note the square grid pattern.

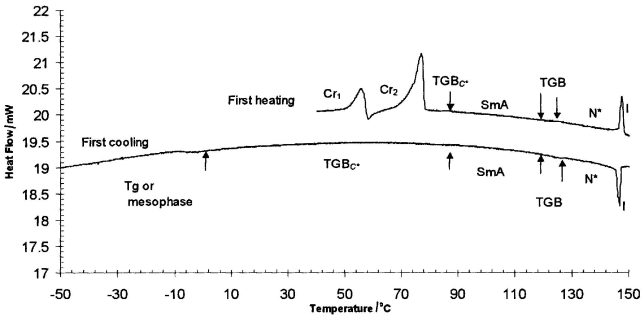

Figure 7. DSC thermograms obtained for the first heating and cooling cycles at a rate of 5°C min^{-1} for the compound **1g**; note that the TGB_{C*} phase exists over a wide temperature range.

The dimer **1g** placed between untreated glass plates, on cooling from isotropic phase, exhibits a focal-conic texture, while on shear the oily streak texture appears which is the characteristic of the N* phase. On further cooling the focal-conic texture of the N* phase shows a filament texture followed by a dark field of view at 115°C that exists till 86°C, indicating the presence of TGB and SmA phases, respectively. At about 85°C the filament pattern remaining in the SmA phase becomes undulated (figure 5) and then remains unchanged till -2.9°C ($\Delta H = 1.01\ \mathrm{J\ g^{-1}}$). The SmA phase on shear gives rise to a planar texture which on further cooling below 85°C yields a square grid pattern (figure 6). This phase remains unchanged till -2.9°C and then changes to either a glassy state or another mesophase, as evidenced by DSC scan (figure 7). On a subsequent (second) heating a step-like variation appears at -2.04°C ($\Delta H = 0.9\ \mathrm{J\ g^{-1}}$) and finally the compound crystallizes at about 32°C ($\Delta H = 7.1\ \mathrm{J\ g^{-1}}$). These observations are highly reproducible.

The characteristic optical features, especially the square grid pattern, have been reported previously for the

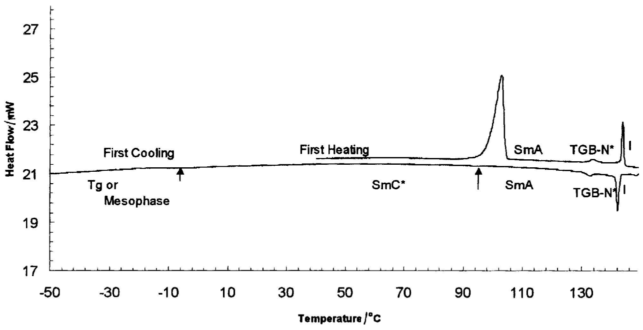

Figure 8. DSC thermograms obtained at a rate of 5°C min^{-1} for the compound **1h** during first heating and subsequent cooling cycles.

TGB_{C*} phase [9]. Thus the dimeric compound **1g**, exhibits a TGB_{C*} phase over a wide temperature range; this observation is significant since to the best of our knowledge the TGB_{C*} phase has been seen only in very few single component systems [9]. The C_{10} homologue **1h**, having a C_5 central alkylene spacer, exhibits enantiotropic SmA, TGB and N* phases while the SmC* is monotropic. This compound also shows a step-like variation at about $-7.0°C$ ($\Delta H = 0.6\ J\ g^{-1}$) that could be due either to the transition from SmC* to a glassy state or to another mesophase which exists till $-40°C$ (figure 8). On subsequent heating, step-like variation appears again at about $-6.2°C$ ($\Delta H = 0.93\ J\ g^{-1}$). On further heating crystal melting is not seen but it crystallizes upon keeping at room temperature for 8–10 h. The relatively low transition temperatures and stability of the SmC* in these compounds is obviously attributable to the presence of difluoro substituents. These fluoro-substituted compounds may also be expected have low viscosity.

In 1975 Meyer *et al.* discovered ferroelectricity in the chiral smectic C (SmC*) phase exhibited by a chiral compound [10] that led to a large number of investigations on such materials, to investigate their chiral properties and to exploit in display applications. It is now well established that ferroelectric liquid crystals (FLCs) are promising candidates for flat panel display technology owing to their fast switching characteristics [11, 12]. However, the commercialization of display devices based on FLCs has had limited success, for many reasons [13]. So far many low molar mass (monomers) and high molar mass FLCs have been reported in the literature [14]. All have been synthesized to stabilize the SmC* phase over a wide temperature range (including room temperature), and to optimize the physical properties such as spontaneous polarization, viscosity, etc. It may be noted that a single component system cannot fulfill all the properties required for device engineering. Thus the liquid crystal medium in a FLC device application is usually a multicomponent system. The mixture may be composed of individual materials that are chiral, or may be made up of an achiral host smectic C mixture that is subsequently doped with chiral component in order to induce ferroelectric (or antiferroelectric) properties in the overall mixture [13]. The dimers **1a**, **1b**, **1e**, **1f**, and **1h** synthesized in the present investigation have stable SmC* phases that could be utilized in FLC device applications either as a single chiral component or as a chiral dopant to an achiral host smectic C.

4. Summary

In this paper we have described the synthesis and thermotropic properties of new unsymmetrical dimers formed by combining a cholesteryl ester moiety covalently to a difluoro-substituted biphenyl core via odd–even flexible alkylene central spacers. The dimer **1a**, having a C_3 spacer and a C_8 terminal alkoxy chain, exhibits enantiotropic SmA, TGB and N* mesophases in addition to a monotropic SmC* phase. The higher homologue **1b**, having a C_{10} terminal alkoxy tail shows enantiotropic SmC* and SmA phases only. The dimers **1c** and **1d**, both having a C_4 central alkylene spacer but differing in the length of terminal alkoxy chain, C_8 and C_{10}, respectively, show enantiotropic SmA, TGB and N* phases. The unsymmetrical dimers **1e** and **1f**, consisting of a C_5-central alkylene spacer but differing in the length of terminal alkoxy tail C_8 and C_{10}, respectively, exhibit enantiotropic SmC*, SmA, TGB and N* phases. The dimeric compound **1g** exhibits an enantiotropic TGB_{C*} phase in addition to SmA, TGB and N* phases. The C_{10} homologue **1h**, having a C_5 central alkylene spacer, exhibits enantiotropic SmA, TGB and N* phases while an SmC* is monotropic. As can be seen, five of the eight unsymmetrical dimers synthesized show either enantiotropic or monotropic SmC* phases. Interestingly in some of the compounds the SmC* exists well below and above room temperature (0–100°C). Thus dimers synthesized in our present investigation stabilize the SmC* phase that can be used in FLC device applications, either as a single chiral component or as a chiral dopant to an achiral SmC host to form a mixture. These molecular assemblies may help in giving a better understanding of the underlying relation between molecular structure and mesomorphic behaviour, and may serve as cheap materials for FLC device technology.

We are grateful to Prof. S. Chandrasekhar for encouraging interest in this work and to Dr S. Krishna Prasad for the helpful discussions. We wish to thank Miss S. Anitha Nagamani for experimental assistance.

References

[1] (*a*) For a recent review on dimers see: Imrie, C. T., and Luckhurst, G. R., 1998, *Handbook of Liquid Crystals*, Vol 2B, edited by D. Demus, J. Goodby, G. W. Gray, H. W. Spiess, and V. Vill (Weinheim: Wiley-VCH), p. 801; (*b*) Emsley, J. W., Luckhurst, G. R., Shilstone, G. N., and Sage, I., 1984, *Mol. Cryst. liq. Cryst. Lett.*, **102,** 223; (*c*) Attard, G. S., Date, R. W., Imrie, C. T., Luckhurst, G. R., Roskilly, S. J., Seddon, J. M., and Taylor, L., 1994, *Liq. Cryst.*, **16,** 529 and references therein; (*d*) Jin, J.-I., Kwon, Y.-W., Yun, Y.-K., Zin, W.-C., and Kang, Y.-S., 1998, *Mol. Cryst. liq. Cryst.*, **309,** 117; (*e*) Ibn Elhaj, M., Skoulios, A., Guillon, D., Newton, J., Hodge, P., and Coles, H. J., 1995, *Macromolecules*, **19,** 373; (*f*) Blatch, A. E., Fletcher, I. D., and Luckhurst, G. R., 1997, *J. mater. Chem.*, **7,** 9.

[2] (*a*) Yelamaggad, C. V., Anitha Nagamani, S., Hiremath, U. S., and Nair, G. G., 2001, *Liq. Cryst.*, **28,** 1009; (*b*) Surendranath, V., 1999, *Mol. Cryst. liq. Cryst.*, **332,** 135; (*c*) Mercelis, A. T. M., Koudijs, A., and Sudholter, E. J. R., 1995, *Liq. Cryst.*, **18,** 843.

[3] Yelamaggad, C. V., Hiremath, U. S., Shankar Rao, D. S., 2001, *Liq. Cryst.*, **28,** 351.

[4] (*a*) Shankar Rao, D. S., Krishna Prasad, S., Raja, V. N., Yelamaggad, C. V., and Anitha Nagamani, S., 2001, *Phys. Rev. Lett.*, **87,** 085504-1; (*b*) Yelamaggad, C. V., 1999, *Mol. Cryst. liq. Cryst.*, **326,** 149; (*c*) Yelamaggad, C. V., Hiremath, U. S., Nair, G. G., and Krishna Prasad, S. (unpublished results); (*d*) Yelamaggad, C. V., Anitha Nagamani, S., Shankar Rao, D. S., Krishna Prasad, S., and Hiremath, U. S., 2001, *Mol. Cryst. liq. Cryst.*, **363,** 1.

[5] (*a*) Jin, J.-I., Kim, H. S., Shin, J.-W., Chung, B. Y., and Jo, B. W., 1990, *Bull. Korea. chem. Soc.*, **11,** 209; (*b*) Hardouin, F., Achard, M. F., Jin, J.-I., Shin, J.-W., and Yun, Y.-K., 1994, *J. Phys. II Fr.*, **4,** 627; (*c*) Hardouin, F., Achard, M. F., Jin, J.-I., Shin, J.-W., and Yun, Y.-K., 1995, *J. Phys. II Fr.*, **5,** 927; (*d*) Hardouin, F., Achard, M. F., Jin, J.-I., Shin, J.-W., and Yun, Y.-K., and Chung, S. J., 1998, *Eur. Phys. J.*, **B1,** 47; (*e*) Cha, S.-W., Jin, J.-I., Laguerre, M., Achard, M. F., and Hardouin, F., 1999, *Liq. Cryst.*, **26,** 1325.

[6] Yelamaggad, C. V., Srikrishna, A., Shankar Rao, D. S., and Krishna Prasad, S., 1999, *Liq. Cryst.*, **26,** 1547.

[7] Hird, M., and Toyne, K. J., 1998, *Mol. Cryst. liq. Cryst.*, **323,** 1.

[8] (*a*) Gray, G. W., Hird, M., Lacey, D., and Toyne, K. J., 1989, *J. chem. Soc. Perkin Trans. II*, 2041; (*b*) Glendenning, M. E., Goodby, J. W., Hird, M., and Toyne, K. J., 2000, *J. chem. Soc. Perkin Trans. II*, 27; (*c*) Hird, M., Goodby, J. W., and Toyne, K. J., 2000, *Proc. SPIE*, **3955,** 15; (*d*) Reiffenrath, V., Krause, J., Plach, H. J., and Weber, G., 1989, *Liq. Cryst.*, **5,** 159; (*e*) Glendenning, M. E., Goodby, J. W., Hird, M., and Toyne, K. J., 1999, *J. Chem. Soc. Perkin Trans. II*, 481.

[9] (*a*) Ribeiro, A. C., Barois, P., Galerne, Y., Oswald, L., and Guillon, D., 1999, *Eur. Phys. J.*, **B11,** 121; (*b*) for a summary on the $\mathrm{TGB}_{\mathrm{C}*}$ phase, see Kitzerow, H. S., 2001, in *Chirality in Liquid Crystals*, edited by H. S. Kitzerow, and C. Bahr (New York: Springer-Verlag); (*c*) Kuczynski, W., and Stegemeyer, H., 1995, *Mol. Cryst. liq. Cryst.*, **260,** 337; (*d*) Kuczynski, W., Stegemeyer, H., 1997, *Proc. SPIE*, **3318,** 90; (*e*) Galerne, Y., 2000, *Eur. Phys. J.*, **E3,** 355; (*f*) Sadashiva, B. K., 1999, *Pramana*, **53,** 213; (*g*) Yelamaggad, C. V., Hiremath, U. S., Shankar Rao, D. S., and Krishna Prasad, S., 2000, *Chem. Commun.*, 57; (*h*) Yelamaggad, C. V., Anitha Nagamani, S., Hiremath, U. S., Shankar Rao, D. S., and Kirshna Prasad, S., 2001, *Liq. Cryst.*, **28,** 1581.

[10] Meyer, R. B., Liebert, L., Strzelecki, L., and Keller, P., 1975, *J. Physique (Lett)*, **36,** L-69.

[11] (*a*) Clark, N. A., and Lagerwall, S. T., 1980, *Appl. Phys. Lett.*, **36,** 898.

[12] Leslie, T. M., 1984, *Ferroelectrics*, **58,** 9.

[13] Goodby, J. W., Toyne, K. J., Hird, M., Styring, P., Lewis, R. A., Beer, A., Dong, C. C., Glendenning, M. E., Jones, J. C., Lymer, K. P., Slaney, A. J., Minter, V., and Chan, L. K. M., 2000, *Proc. SPIE*, **3955,** 2.

[14] (*a*) Furukawa, K., and Terashima, K., 1986, European Patent Application, EP178647; (*b*) Keller, P., 1984, *Mol. Cryst. liq. Cryst.*, **102,** 295; (*c*) Chen, Y., and Wu, W.-J., 1998, *Liq. Cryst.*, **25,** 309; (*d*) Dingemans, T. J., Poon, C.-D., and Samulski, E. T., 1998, *Liq. Cryst.*, **24,** 247.